MINERAL CHEMISTRY OF ASBESTOS BEARING ULTRAMAFITES AND ASSOCIATED ROCKS FROM HOLENARASIPUR SCHIST BELT

R. V. RAGHAVENDRA, G. V. ANANTHA IYER AND

T. R. NARAYANAN KUTTY

(*Department of Inorganic and Physical Chemistry, Indian Institute of Science, Bangalore-560012*)

Received on May 4, 1976 and in revised form on August 17, 1976

ABSTRACT

The predominant variety of asbestos from Holenarasipur schist belt is anthophyllite. It is derived from the ultramafic rocks which are associated with amphibolites metapelites and TAAC (tremolite-actinolite, anthophyllite, chlorite) schist. Amphibolites contain tschermakite-hastingsite hornblende of Fe/Fe+Mg ratio 0·55 *to* 0·35. *Plagioclase from the amphibolites have unusually high Ca content, in the range of* An_{40} *to* An_{60}. *Some of the amphibolites have garnets with uncommon end member content of* alm_{70}-py_{15}-gr_{15}. *Anthophyllites contain less than one Al atom per unit formula. They have incoherent FeO/MnO ratio and variable CaO and* Na_2O. *Chlorites have high mg-component* (0·75 *to* 0·90); *non-uniform Si/Al ratio ranging from talc-chlorite to clinochlore. Staurolite and garnet from metapelites have Fe-component more than* 0·85. *Olivines from ultramafites range from* Fo_{80} *to* Fo_{90}; *their low Ca, Mn content and high* Al_2O_3 *indicate that the ultramafites are intrusives. Mineral chemistry of TAAC schists correspond to a mixed rock type of metapelite and ultramafites ranging from dunite, harzburgite to lherzolite. The metamorphic reactions in ultramafites and the contaminated rocks were accompanied by* CO_2 *metasomatism, which accounts for the serpentine-anthophyllite coexistence. P-T conditions of metamorphism correspond to upper green schist to lower amphibolite facies, higher pressures, not commonly encountered in the continental types. Anthophyllite acquires fibrous morphology by recrystallisation in* CO_2 *rich fluid towards the waning stages of metamorphism. Minor elements and directional pressures may have been additional factors for the development of asbestiform morphology.*

Key words: Asbestos, Anthophllite, Ultramafites, high pressure amphibolites.

1. INTRODUCTION

Asbestos from the schist belt near Holenarasipur, Hassan District, Karnataka, has been differently identified as tremolite, chrysotile and anthophyllite.

A preliminary report on the asbestos from Mangalapur, presented elsewhere [1], indicates that anthophyllite is the predominant variety and is derived from ultramafic rocks. A systematic study of asbestos and the coexisting minerals from this schist belt has since then been completed; mineral chemistry and its significance is discussed in this paper.

2. GEOLOGY AND ROCK TYPES

Geology of Holenarasipur schist belt has been described by many of the previous investigators [2–5]. The major part of this Y-shaped schist belt is covered by dark amphibolites. Asbestos bearing ultramafites occur as random patches, mostly restricted to the region, south of the river Hemavathi, as shown in Fig. 1. They are associated with tremolite-actinolite schist, hornblende schist and metapelites; the surrounding rocks being Peninsular gneisses.

Ultramafic bodies are of different sizes, the largest one being seen to the east of Tirumalapur. They are conformably enclosed by tremolite-actinolite and hornblende schists. However, the ultramafites are not always folded in conformity with the schist. Instead of the contact metamorphic effects with the enclosing rocks, there are zones of reactions between ultramafites and other rock types. Ultramafites are so highly altered that the only criterion which can be used in classifying the rock types is the chemical composition. The lithological units are briefly described below.

Amphibolites (hornblende schists).—The dark hornblendic rocks representing flows, agglomerates and tuffaceous layers of original basaltic composition appear as thick sheets in the northern part of the schist belt. Most of the amphibolites are schistose type; massive ones being not uncommon. In the southern part, amphibolites are associated with ultramafites, particularly on the western flanks of Tirumalapur hill. Since meta-anorthosite patches are observed at places in conformable association with these amphibolites, at least some of the exposures may be derived from the original gabbroic rocks. Generally the amphibolites contain 80–90% hornblende (in places, monomineralic), 5–20% plagioclase and 0–5% quartz. There is a second variety of amphibolite containing porphyroblastic garnets, typical exposures of which are seen on the eastern hillock facing the asbestos mine at Mangalapur and on the western margin of Idegondanahalli area. This rock type contains 70–80% hornblende, 10–15% plagioclase, 5–15% garnet and 5–10% quartz.

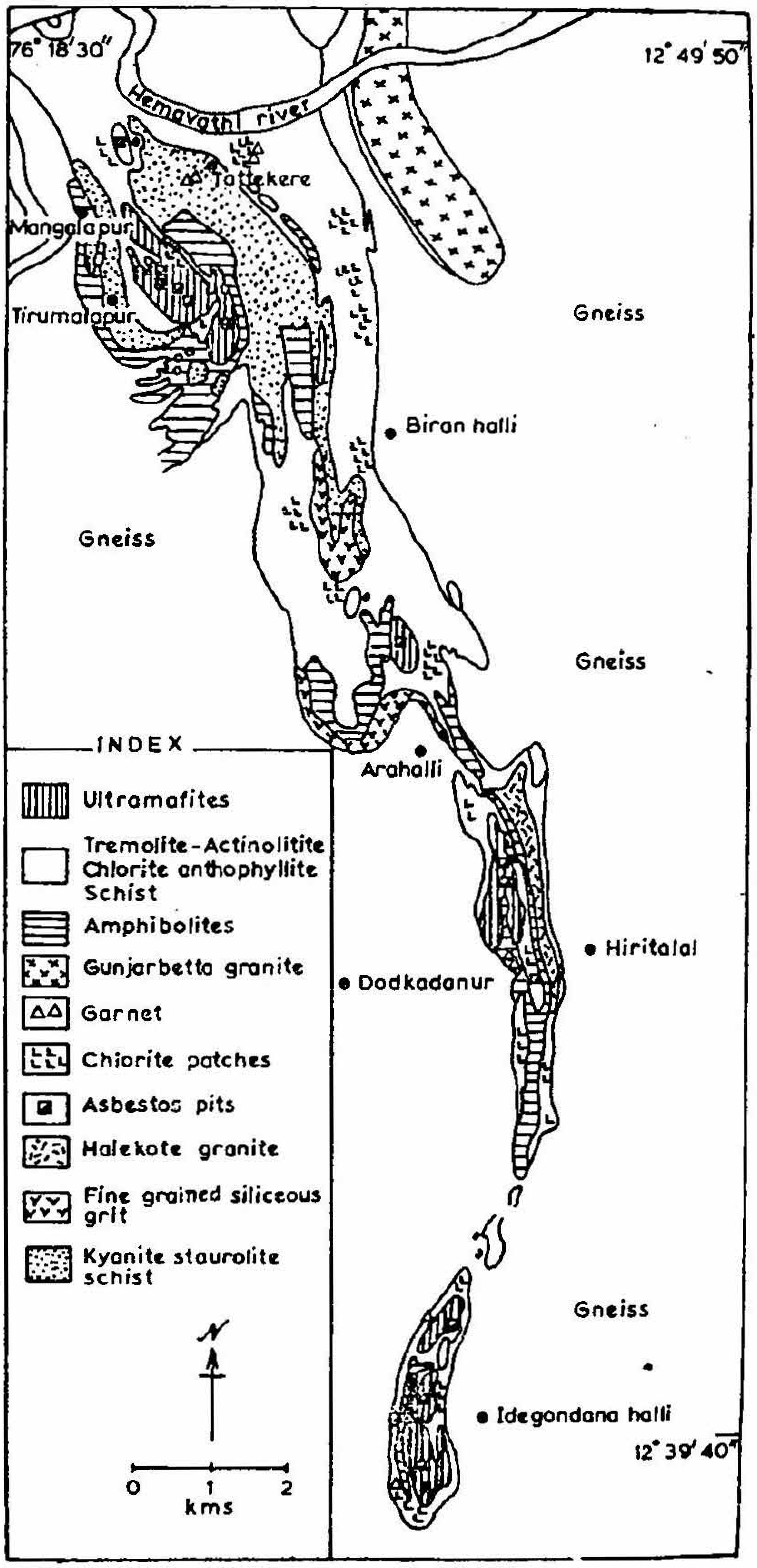

FIG. 1. Geological map of the southern portion of the Holenarasipur schist belt. After Rama Rao, B. [3].

Whole rock composition of amphibolites (Table I) show high CaO (9–13%) and alkali (1–5%), with variable alumina content (13–20%). Non-garnetiferous amphibolites have Ca/Al ratio (atom) in the range of 1·11 to 1·33, while the garnetiferous ones have lower values (0·37 to 0·59). Mg/Mg + Fe ratio (atom) ranges from 0·35 to 0·5 for amphibolites. Chromium (90–150 ppm) and nickel (100–150 ppm) contents are much lower than those of ultramafites.

Ultramafites.—Ultramafites are altered considerably and have different paragenesis:

(*a*) Nearly unaltered dunites with 85–90% olivine and minor serpentine. This rock type is comparatively rare.

(*b*) Tough and compact ultramafic rocks, often appearing as a dyke, contain 5–10% olivine, 30–50% antigorite, 20–30% magnesite, 5–15% anthophyllite, 10–15% talc and 0–5% magnetite. A variant of the same rock is seen near Tattekere, containing insignificant amount of olivine, rounded porphyry crystals of magnesite, fibrous talc (picrolite), serpentine and minor magnetite. The weathered surface of this rock shows cavernous appearance.

(*c*) Serpentinites with antigorite as the major constituent. The rocks contain magnetite as dispersed fine grains which impart dark appearance. They are interspersed with short cross-fibres of chrysotile. Chromite is a minor phase in this rock.

(*d*) Anthophyllite exposures are randomly encountered in the ultramafites, with morphology ranging from massive to asbestiform. Crystalline dolomite and magnesite are associated with anthophyllite in some exposures.

The ultramafic rocks are characterised by high MgO, low CaO, alkal and alumina (Table I). Irrespective of the kind of alteration, Mg/Mg + Fe ratio (atom) is maximum for ultramafites (0·80 to 0·9). They have high Cr (1000–2500 ppm) and Ni (1500–3000 ppm). CO_2 and H_2O are variable.

Metapelites.—The important exposures of this rock type are found east of Tirumalapur hill. Well-developed euhedral crystals of blue-kyanite, staurolite, garnet and massive semi transparent quartz are the characteristic minerals of metapelites. Relative abundance of individual minerals vary from place to place. Except the minor phase of muscovite or sericite as alteration product of kyanite, alkali-bearing minerals are absent (excluding the muscovite in the pegmatites). Kyanite bearing quartzites are found in Tattekere and down south areas.

TABLE I

Composition of whole rocks

	1	2	3	4	5	6	7	8	9	10
SiO_2	53·51	42·12	49·62	27·88	38·85	38·66	37·72	36·57	46·68	53·51
TiO_2	0·54	0·90	1·28	..	..	..	0·01	..	traces	0·54
Al_2O_3	12·35	14·27	15·55	4·64	1·35	0·41	2·35	1·43	7·96	13·25
Fe_2O_3	4·99	6·03	3·55	..	2·07	2·37	5·13	8·03	1·44	4·99
FeO	6·99	16·84	14·68	9·67	12·37	8·08	3·47	2·74	8·20	6·99
MnO	0·05	0·10	1·30	0·01	0·02	0·01	0·40	0·01	0·06	0·05
MgO	5·43	3·63	5·04	36·68	37·19	36·09	36·10	38·07	22·04	5·43
CaO	11·76	11·79	5·88	0·23	0·23	0·50	0·10	0·57	6·73	11·76
Na_2O	1·76	2·20	1·24	0·21	0·04	0·19	0·14	0·05	0·37	1·76
K_2O	0·34	0·04	0·03	0·09	0·02	0·04	0·06	0·01	0·08	0·34
H_2O^+	0·92	1·08	1·31	13·32	7·05	12·09	12·54	10·12	6·01	0·92
H_2O^-	0·01	0·23	0·09	0·67	0·23	0·90	0·96	0·18	0·10	0·01
CO_2	..	..	..	5·83	..	..	0·33	0·64	..	..
Total	99·54	99·23	99·57	99·23	99·42	99·34	99·31	99·02	99·67	99·54
Cr (ppm)	126	101	142	1822	2010	2291	2232	1968	378	126
Ni (ppm)	186	166	178	2431	3025	2965	3134	2621	436	186
Mg/Mg + Fe (atom)	0·41	0·23	0·34	0·87	0·82	0·86	0·89	0·87	0·81	0·41
Ca/Al (atom)	1·2	1·11	0·51	0·07	0·22	1·64	0·06	0·05	1·14	1·2

*Simplified norm**

Ab	17	10	10	..	..	..	..	..	..	15
An	29	32	28	3	..	..	..	6	23	18
Di-He	44	28	50	..	..	..	..	..	11	13
Oliv	..	22	..	75	77	69	66	83	14	23
En-Hy	4	..	..	..	22	31	31	10	52	41
Neph	..	8	..	..	..	..	..	..	..	..
Mt	..	..	..	16	..	..	..	..	..	..
Cor	..	..	3	6	1	..	3	1	..	..
Qz	6	..	9	..	..	..	..	..	..	..
Felsic	52	42	50	9	1	0	3	6	23	23
Mafic	48	58	50	91	99	100	97	93	77	77

1. I_8 Amphibolite, Idegondanahalli
2. Y_H Amphibolite, Tirumalapur.
3. T_{2G} Garnetiferous amphibolite, Tirumalapur.
4. M_{12} Olivine-antigorite-anthophyllite,–breunnerite-magnetite, ultramafite, Mangalapur.
5. Y_{14} Olivine-antigorite-anthophyllite-magnetite, ultramafite, Tirumalapur.
6. OT Antigorite-magnetite, Tirumalapur
7. I_{16} Antigorite-chrysotile-magnetite, ultramafite, Idegondanahalli.
8. I_{10} Antigorite-magnetite, ultramafite, Idegondanahalli.
9. ITCh Tremolite-chlorite, TAAC rock, Idegondanahalli.
10. I_{14} Tremolite-chlorite-anthophyllite, TAAC, rock, Idegondanahalli.

* Simplified norms calculated on the anhydrous basis (without CO_2 and H_2O).

Due to the coarse nature and non-uniform distribution of the minerals, composition of the whole-rock could not be determined. In general, they have high SiO_2 and Al_2O_3, variable FeO–MgO contents ($FeO >> MgO$) and low CaO as well as alkalies.

Tremolite-actinolite-anthophyllite-chlorite schists (TAAC schists).—Tremolite-actinolite schists are the predominant rock type in this category. The earlier maps represent them by the same name. However, chlorites have greater preponderance in this rock type, occurring as foliated sheets, lenses or monomineralic schistose rock, containing euhedral garnets. Kyanite, staurolite and magnetite crystals are found randomly distributed in the chlorite-anthophyllite schists. They may be monomineralic with respect to any one of the constituents. TAAC schists of Idegondanahalli and Dodkadanur have characteristic porphyritic crystals, now altered to tremolite-anthophyllite-chlorite. Asbestiform tremolite occurs in Dodkadanur along with anthophyllite asbestos. Magnesite and dolomite are occasionally encountered.

Chemical composition of TAAC schists are variable, depending upon the relative proportion of actinolite, chlorite and anthophyllite (Table I). They may be represented by the constituents: SiO_2-Al_2O_3-MgO-FeO-H_2O-CO_2, with low alkali and TiO_2. $Mg/Mg + Fe$ is lower in the actinolite-chlorite rocks than that of anthophyllite-bearing ones. Cr (350–450 ppm) and Ni (400–600 ppm) contents are intermediate between those of ultramafites and amphibolites.

3. MINERAL CHEMISTRY

Chemical analysis has been carried out by the wet methods. SiO_2 is determined gravimetrically after sodium carbonate fusion; alumina, total iron, calcium and magnesium by complexometry; titania and manganese colorimetrically and the alkali elements by flame photometry. Ferrous iron is estimated by the vanadate method of Wilson [6]. Water and carbon dioxide are determined by absorbing in magnesium perchlorate and ascarite respectively.

Calcic amphiboles.—Ca-amphiboles from the amphibolite rocks are either hornblendes or actinolitic hornblendes, while those from TAAC schists are actinolites or tremolites (Table II). Fe-content is maximum in hornblendes from amphibolites. TiO_2, Na_2O, K_2O and Al_2O_3 show marked variations in Ca-amphiboles from the above-mentioned rock types,

TABLE II

Chemical composition of calcic amphiboles

	72	73	74	75	76	77	78	79	80	83	85	87	90
SiO_2	56·05	54·70	55·80	56·49	55·41	54·16	52·60	52·09	51·60	40·91	39·36	40·21	43·20
TiO_2	0·00	0·00	0·10	0·08	0·06	0·00	0·34	0·67	0·68	2.56	1·93	1·50	0·09
Al_2O_3	1·77	3·45	3·95	1·28	1·02	3·10	7·14	7·55	7·76	22·34	16·57	12·87	19·63
Fe_2O_3	0·22	0·18	0·00	0·97	1·83	2·30	4·89	3·56	2·85	0·15	6·15	5·33	1·01
FeO	2·79	8·44	3·85	7·39	6·90	9·01	10·07	9·73	11·81	15·58	15·05	16·50	15·09
MnO	0·42	0·00	0·23	0·11	0·13	0·25	0·28	0·29	0·22	0·01	0·01	0·03	0·12
MgO	23·89	19·24	22·31	20·46	19·11	18·75	10·68	12·42	11·45	2·82	7·06	8·51	5·24
CaO	11·63	11·67	11·12	10·31	11·43	9·53	10·65	10·09	9·65	11·20	11·02	10·39	11·20
Na_2O	0·39	0·27	0·32	0·45	0·42	0·30	0·84	0·94	1·35	1·45	1·71	1·47	1·60
K_2O	0·14	0·04	0·10	0·16	0·11	0·11	0·38	0·35	0·16	0·33	0·94	0·21	0·29
H_2O^+	2·35	1·98	2·14	2·26	2·47	2·28	2·03	1·84	2·21	1·89	1·98	2·34	2·15
H_2O^-	0·04	0·13	0·10	0·17	0·32	0·20	0·23	0·56	0·18	0·09	0·02	0·00	0·16
Total	99·69	100·10	100·00	100·13	100·11	100·05	100·13	100·19	99·92	99·93	100·38	100·42	99·78

TABLE II (*Contd.*)

Number of ions on the basis of 24 (0) *atoms*

	72	73	74	75	76	77	78	79	80	83	85	87	90
Si	7·690	7·681	7·661	7·866	7·745	7·633	7·526	7·452	7·398	6·032	5·860	5·990	6·328
Al^4	0·270	0·319	0·339	0·134	0·255	0·367	0·474	0·548	0·602	1·968	2·140	2·010	1·672
Al^6	0·000	0·252	0·296	0·076	0·061	0·148	0·729	0·682	0·709	1·914	0·770	0·250	1·717
Ti	0·000	0·000	0·010	0·008	0·006	0·000	0·037	0·072	0·073	0·284	0·220	0·170	0·009
Fe^{3+}	0·023	0·019	0·000	0·010	0·193	0·246	0·526	0·381	0·307	0·015	0·540	0·600	0·111
Fe^{2+}	0·321	0·997	0·442	0·861	0·806	1·062	1·206	1·164	1·417	1·958	1·400	2·010	1·849
Mn	0·049	0·000	0·027	0·013	0·015	0·030	0·034	0·035	0·027	0·001	0·001	0·003	0·015
Mg	4·886	4·028	4·566	4·247	3·981	3·940	2·274	2·650	2·446	0·620	1·601	2·038	1·144
Ca	1·714	1·759	1·638	1·540	1·714	1·441	1·635	1·548	1·485	1·778	1·780	1·602	1·760
Na	0·104	0·074	0·085	0·122	0·114	0·082	0·233	0·261	0·375	0·414	0·490	0·420	0·454
K	0·025	0·004	0·018	0·028	0·020	0·020	0·069	0·004	0·029	0·062	0·180	0·050	0·054
(OH)	2·24	1·86	1·96	2·10	2.30	2·15	1·94	1·75	2·11	1·86	1·96	2·33	2·10

72.	D_4	, Tremolite, TAAC schist, Dodkadanur.
73.	M_{17}	Actinolite, TAAC schist, Mangalapur.
74.	$I_{26\cdot a}$	Actinolite, TAAC schist, Idegondanahalli.
75.	T_{26}	Actinolite, TAAC schist, Tirumalapur.
76.	T_{28}	Actinolite, TAAC schist, Tirumalapur
77.	T_{29}	Actinolite, TAAC schist, Tirumalapur.
78.	T_{30}	Actinolitic hornblende, amphibolite, Tirumalapur.
79.	T_{31}	Actinolitic hornblende, amphibolite, Tirumalapur.
80.	T_{32}	Actinolitic hornblende, amphibolite, Tirumalapur.
83.	I_7	Hornblende, garnetiferous amphibolite, Idegondanahalli.
85.	D_{12}	Hornblende, garnetiferous amphibolite, Dodkadanur.
87.	T_4	Hornblende, amphibolite, Tirumalapur.
90.	$T_{a\cdot 32}$	Hornblende, amphibolite, Tattekere.

Considering the classification of Ca-amphiboles, Fig. 2 (*a*) and (*b*) show the compositions plotted in the diagrams of Deer *et al.* [7]. Those falling in field I are tremolites and actinolites from TAAC schist. They have less than 0·5 atoms of tetrahedral Al, low (Na + K) and (Al^6 + Fe^{3+} + Ti). Ca-amphiboles from the foot-hills of Tirumalapur, plot in the intermediate field with 0·5–1·0 atom of Al^4, 0·25–0·4 atoms of (Na + K) and 1·0–1·3 atoms of (Al^6 + Fe^{3+} + Ti). They can be classified as actinolitic hornblendes. Amphiboles falling in field II have definite bias to

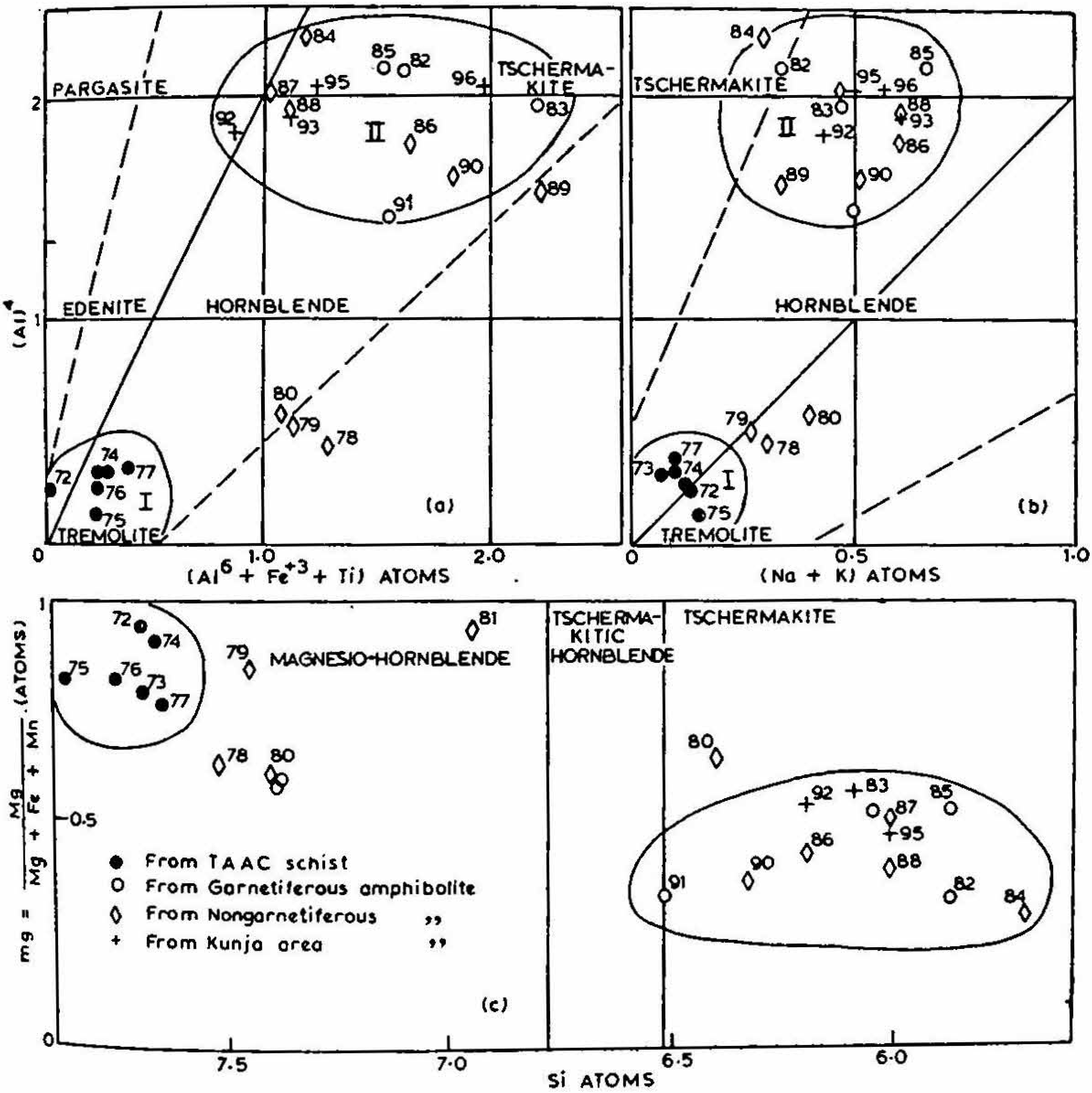

FIG. 2. Classification of calcium amphiboles. The molecular ratio calculated on the basis of 24(0) atoms. The normal limits of calcium amphiboles are shown by broken lines. 2 (*a*) and (*b*) after Deer *et al.* [7]. Fig. 2 (*c*) after Leake [8].

tschermakites Fig. 2 (*a*). Composition of Ca-amphiboles from garnetiferous as well as garnet-free amphibolites fall in the same field. A few amphiboles from the northern part of the schist belt (Kunja area) are included in Fig. 2 for comparison. The extent of Mg-Fe substitution is represented as a function of Si atoms per molecule in Fig. 2 (*c*) following Leake [8]. This diagram is applicable to amphiboles with less than 2·5 atoms of (Ca + Na + K) and 0·5 atoms of Ti. This criterion is satisfied by all the amphiboles from the schist belt. Those from TAAC schist have high Si atoms (7·5–8·0) and mg-ratio. They plot in the magnesiohornblende field. Amphiboles from Tirumalapur, classified as actinolitic-hornblendes in Fig. 2 (*a*) and (*b*), also fall in the same field. All the other amphiboles plot in the tschermakite field and have mg-ratio varying from 0·30 to 0·55. Hence they are to be named as ferro-tschermakites.

The interelemental relations in amphiboles are very peculiar. Figure 3 (*a*) shows the relation between Ti and (Na + K) atoms which divides the amphiboles into three types. (i) low Ti and (Na + K) for those from TAAC schists; (ii) low Ti and variable (Na + K) for one set of hornblendes; (iii) both Ti and (Na + K) high, for a second set of hornblendes. The separation of hornblendes into two distinct groups indicates that the amphibolites are derived from more than one parent rock, say gabbros and basaltic lavas. Since the amphiboles from garnetiferous rocks fall in both the fields, unequivocal demarcation is not possible on the basis of mineral chemistry of amphiboles. Figure 3 (*b*) shows the correlation of FeO *vs.* TiO_2, separating the amphiboles into three groups. Irrespective of the FeO content, TiO_2 in actinolites is very negligible. Figure 3 (*c*) shows the relation of FeO and MnO, where no geochemical coherence is shown up, unlike that envisaged by Kostuk and Sobolev [9]. MnO content in the actinolites shows widest variation for a given range of FeO. Comparing Fig. (3*b*) and (3*c*,) it is evident that TiO_2-rich hornblendes fall in low MnO field. Such inter-elemental relations in Ca-amphiboles can only be explained on the basis of disturbances in bulk chemistry of rocks, essentially due to the mixing of more than one rock type prior to metamorphism.

Anthophyllite.—Anthophyllites exhibit different morphology. Of these the important varieties are massive forms containing transparent acicular crystals, asbestiform of varying fibre diameter and the semi-crystalline 'mountain wood' type. X-ray powder pattern of all the morphological forms can be indexed on the basis of orthorhombic unit cell.

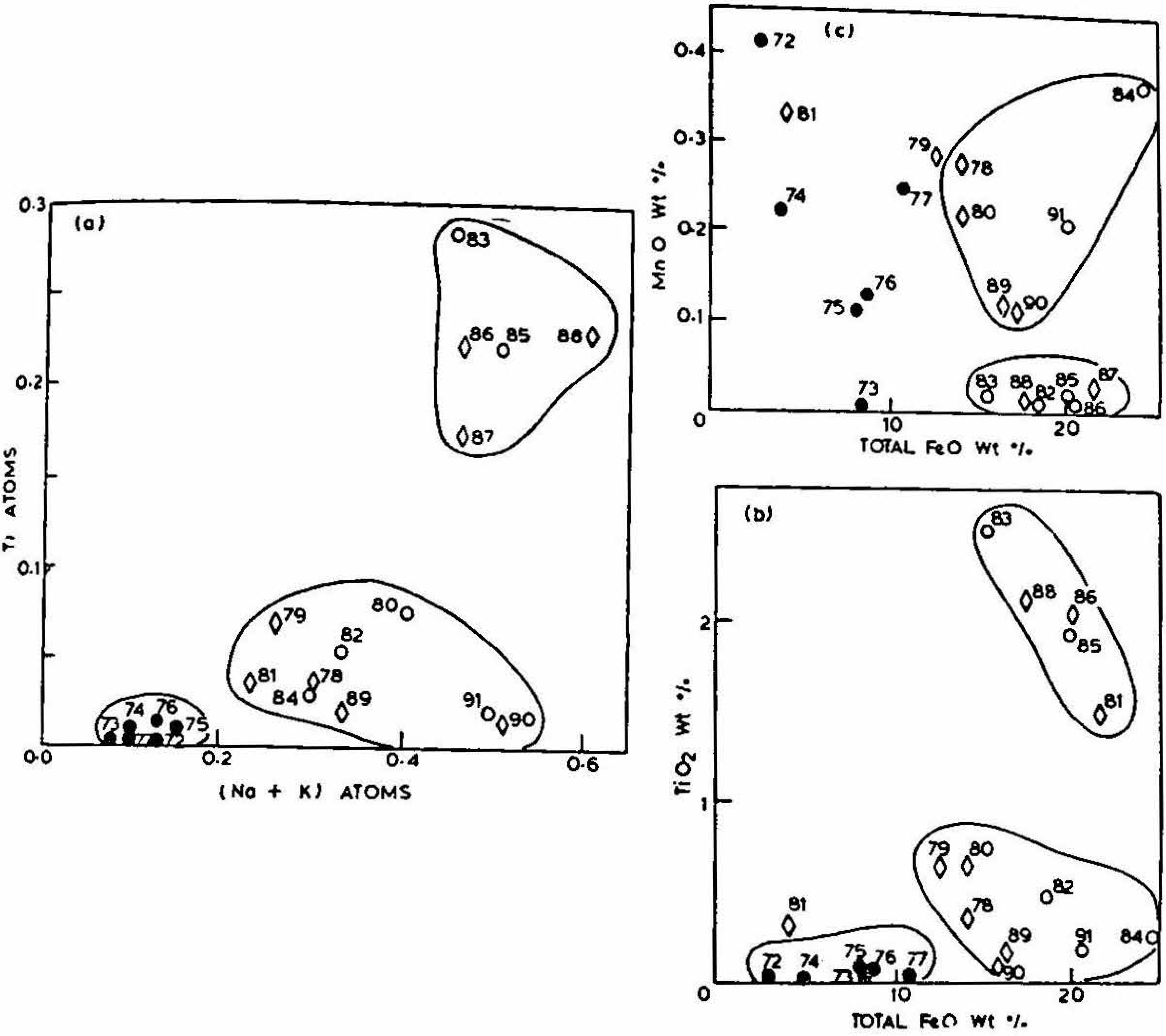

FIG. 3. Interelemental relations in calcic amphiboles. (*a*) (Na + K) *vs.* Ti atoms, (*b*) Total FeO *vs.* MnO wt %, (*c*) Total FeO *vs.* TiO_2 wt %, Symbols are as in Fig. 2.

Major compositional variation in anthophyllites is through the substitution : Mg + Si ⇆ 2Al, leading to the Al-rich end member, gedrite. However, in the present case, increase in Al_2O_3 content is found not proportional to lowering MgO (Table III). Substitution of Si by Al is restricted to less than one atom per molecule. Thus, the orthoamphiboles range upto the middle member of anthophyllite-gedrite series.

Figure 4 (*a*) gives the relation of Si atoms with 100 Mg/Mg + Fe + Mn. Asbestiform anthophyllites have minimum tetrahedral Al (0·0–0·4 atoms) and wider range of Mg/Mg + Fe ratios. Massive anthophyllites, on the

TABLE III

Chemical composition of anthophyllites

	17	20	25	30	31
SiO_2	56·25	46·60	53·50	51·46	57·70
Al_2O_3	0·85	9·74	2·15	..	2·78
Fe_2O_3	1·53	2·50	6·31	13·22	0·21
FeO	7·64	4·99	3·54	7·67	7·42
MnO	0·48	0·53	0·20	..	0·40
MgO	26·95	29·62	23·46	20·89	26·03
CaO	0·48	0·95	5·55	1·68	0·56
Na_2O	0·92	1·20	0·24	0·10	0·62
K_2O	0·09	0·04	0·20	0·14	0·10
H_2O^+	4·01	2·96	3·42	3·40	3·41
H_2O^+	0·42	0·58	1·31	0·93	0·56
Total	99·62	99·71	99·88	99·49	99·79
	Number of ions on the basis of 24 (0) *atoms*				
Si	7·632	6·424	7·416	7·401	7·756
Al^4	0·136	1·581	0·351	..	0·244
Al^6	..	..	..	..	0·196
Fe^{3+}	0·156	0·259	0·658	1·431	0·021
Fe^{2+}	0·867	0·575	0·326	0·923	0·834
Mn	0·055	0·061	0·023	..	0·046
Mg	5·390	6·087	4·848	4·307	5·216
Ca	0·042	0·141	0·825	0·259	0·081
Na	0·241	0·321	0·064	0·028	0·162
K	0·015	0·007	0·035	0·029	0·017
(OH)	3·63	2·72	3·16	3·07	3·06

17. Y. Monntainwood, Yenneholeranganabetta, Tirumalapur.
20. Y_1 Medium gedrite Yenneholeranganabetta, Tirumalapur.
25. I_4 Calcic asbestos, Idegondanahalli.
30. M_6 Asbestos associated with dolomite, Mangalapur,
31. T_{1a} Massive anthophyllite, Tirumalapur.

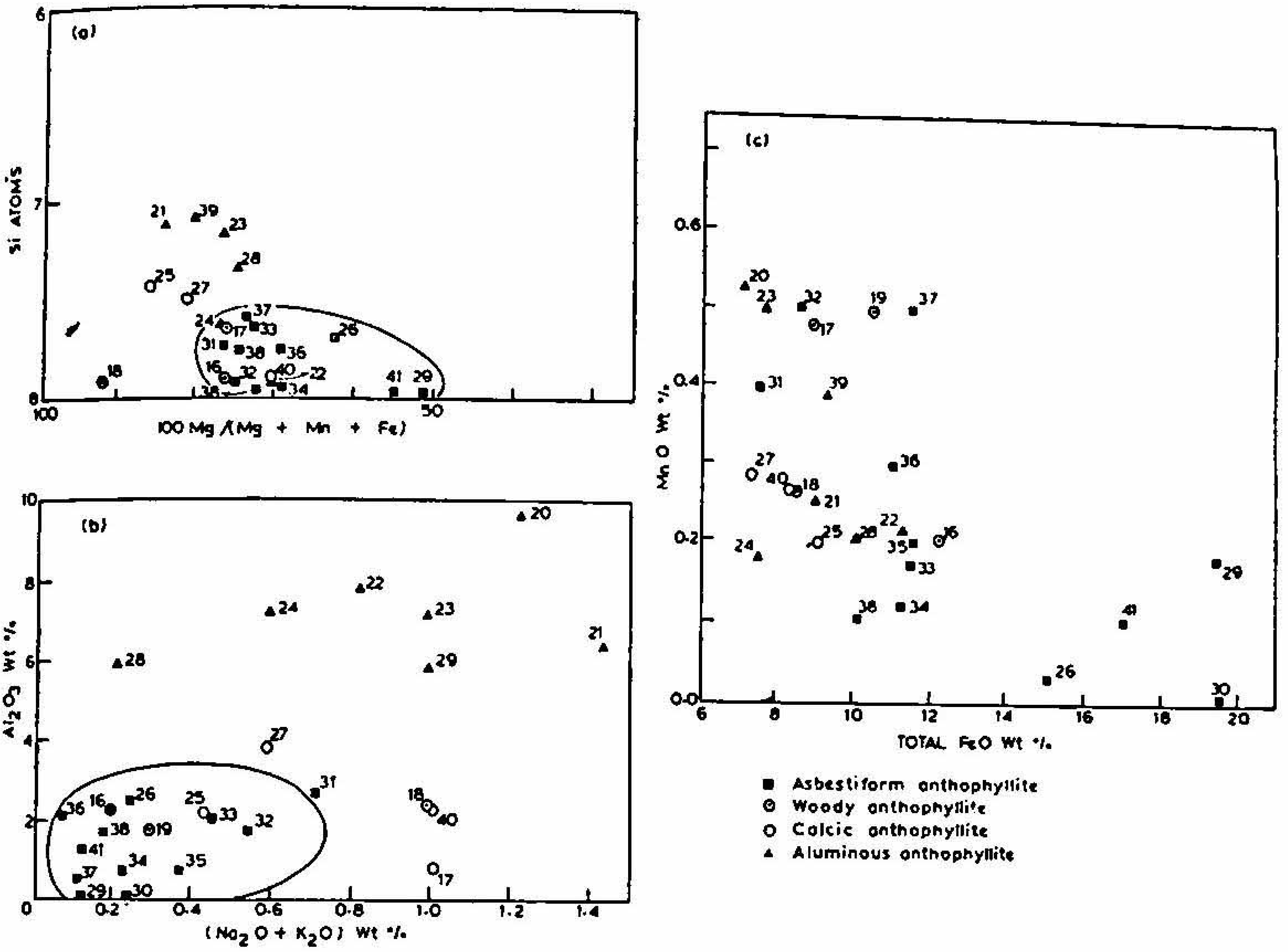

FIG. 4. Interelemental relations in anthophyllites. (*a*) 100 Mg/Mg + (Mn + Fe) *vs.* Si atoms, (*b*) (Na_2O + K_2O) *vs.* Al_2O_3 wt %, (*c*) Total FeO *vs.* MnO wt %

other hand, have restricted Mg/Mg + Fe ratio, with higher Al^4. Figure 4 (*b*) shows the approximate correlation between Al_2O_3 and total alkali content where the anthophyllite asbestos plot near the origin of the figure. The geochemical correlation between FeO and MnO in anthophyllites is found to be poor, as shown by the spread of points in Fig. 4 (*c*). For a narrow range of 8–12 wt% of FeO, MnO content varies from 0·1 to 0·6.

Figure 5 (*a*) shows the composition of anthophyllites plotted on the ACF diagram. The asbestiform, plots close to the F corner, indicating that-CaO and Al_2O_3 should be a minimum for the persistence of fibrous morphology. Anthophyllites from TAAC schists have maximum CaO content, demonstrating the influence of rock composition on the extent of Ca-substitution. Beyond a certain limit of CaO, conversion to monoclinic, Ca-amphibole takes place. Anthophyllites plotting near the AF line are those coexisting with chlorites, in the vicinity of ultramafites.

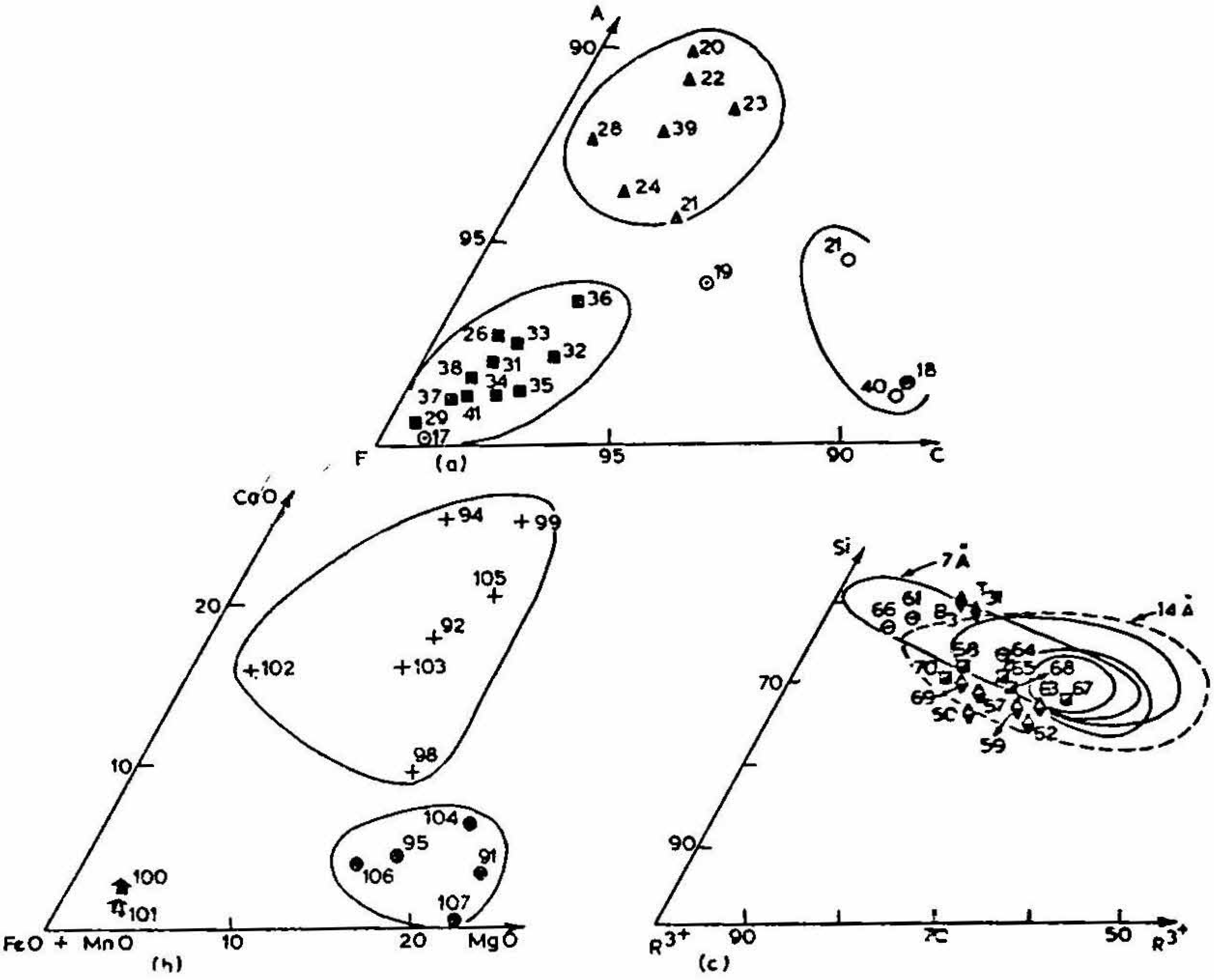

FIG. 5. Compositional variations in anthophyllites, garnets and chlorites. (*a*) Anthophyllites plotted on ACF diagram. Symbols are as in Fig. 4. A = $Al_2O_3 - (Na_2O + K_2O)$, C = CaO and F = (FeO + MnO), (*b*) Mole proportions of CaO, FeO + MnO and MgO in garnets from amphibolites (+), chlorites (●) and metapelites (†), (*c*) ACF for chlorites $R^{2+} = (MgO + FeO + MnO)$, $R^{3+} = Al_2O_3 + Fe_2O_3$, Si = SiO_2. Contours indicate different temperatures of stability, increasing towards the center. Chlorites coexisting with anthophyllites close to the ultramafites ⊙, chlorites from TAAC schist, ☐ chlorites from, TAAC schist, near the metapelites △, chlorites from the metapelites (northern part of the schist belt Singarahalli) ▲.

The number of (OH) groups per formula varies for different morphological forms, in the decreasing order mountain wood type > asbestiform > massive form. Water content is said to influence the mechanical properties of asbestos.

Chlorite.—X-ray diffraction pattern of the chlorites reveal that they are 14 Å (II *b*) poly type. It indicates that they are of metamorphic origin and not the low temperature alteration products.

Table IV gives a few selected analyses. Mineral chemistry of chlorites is explained on the basis of substitution in hypothetical talc, $Mg_6Si_8O_{20}(OH)_4$ and brucite, $Mg_6(OH)_{12}$ layers with which the chlorite structure is built up. Substitution of Si by Al in the tetrahedral sheets imparts negative charge and is compensated by the substitution of Al and Fe^{3+}, in the octahedral sheets of both talc and brucite layers. Classification of chlorites by Hey [10] is based on these substitutions. Figure 6 shows that the chlorite fall in talc-chlorite, penninite, clinochlore and sheridanite fields. Talc-chlorite, found as relict nodules in the asbestos horizons are unstable when compared to the more aluminous chlorites. In the TAAC schist, all the chlorites encountered are either sheridanite or clinochlore. Mg/Mg + Fe ranges from 0·75 to 0·9 in chlorites. Chlorites coexisting with staurolite and garnet are poorer in Mg, than those from the vicinity of ultramafites.

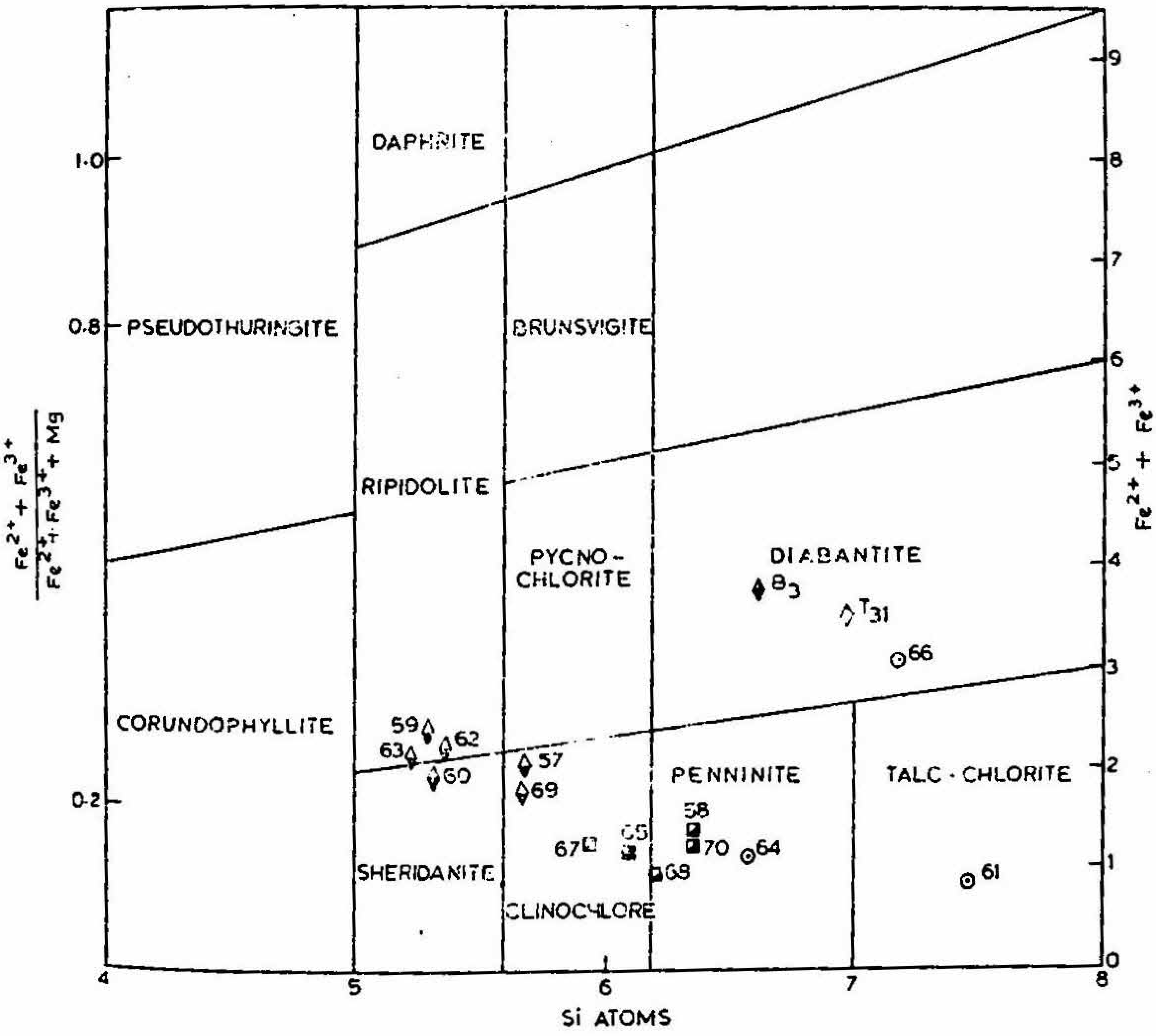

FIG. 6. Classification of chlorites following Hey, M. H. [10].

As mentioned by Velde [11], the ratio of Si, R^{2+} and R^{3+} ions is an indicator of the stability ranges of chlorites. Figure 5 (*c*) shows the relation of these values for the present chlorites. The most probable compositional ranges for low temperature. 7 Å chlorites and higher temperature 14 Å chlorites are delineated in the figure. All the chlorites fall in the latter field. R^{3+}/R^{2+} ratio for the octahedral ions varies from 0·08 to 0·35. Since the major R^{2+} ion is Mg, the thermal stability of chlorites extends to higher temperature ranges, particularly when they are trioctahedral chlorites as shown by the full occupancy of 12·0 to 12·6 in the octahedral layers.

Garnets.—The garnet compositions are sensitive to whole rock chemistry as well as the P–T conditions of formation. Garnets coexisting with chlorite in TAAC schist are mostly almandine-pyrope, with the end member contents: alm: 63–72, py: 14–22, and: 4–11, gr: 0–2, sp: 3–16. MnO is the highly variable constituent in them (Table V). Garnets coexisting with kyanite and staurolite are mostly Fe-rich, with alm: 88–90, py 7–8, and: 0–4, gr: 0–1, sp: 0–2. In comparison, garnets from amphibolites have higher CaO content and wider composition ranges. The general range of end member content may be given as alm: 59–77, py: 10–15 and 0–7, gr: 15–20, sp: 1–8. Such alm-py-gr garnets indicate higher pressure of formation.

Figure 5 (*b*) shows the relation of Ca-(Fe + Mn)–Mg in garnets, which plot in three different fields. Those from metapelites plot near (Fe + Mn) corner. Garnets from TAAC schist plot on (Fe + Mn)–Mg line, with minimum Ca-content. Those from amphibolites have a larger compositional field.

Olivine.—Olivines are Mg-rich, with the composition ranging from FO_{90} to Fo_{82} (Table VI). There is good identity in the Mg/Fe ratio of the ultramafic rocks of various mineral assemblages and that of the olivine in them. Simkin and Smith [12] showed that the minor elements in olivines from terrestrial rocks have limited compositional variation. They have divided the olivine into two groups, depending upon the Ca-content. Those from extrusive and hypabyssal rocks have more than 0·1% Ca. Olivines from plutonic rocks have Ca-content less than 0·1%. The present olivines correspond to the second group. Mn-content is less than 0·05% and the concentration of Ni is comparatively large (upto 0·5%). Higher Al_2O_3 content in them is said to indicate higher temperature of crystallisation.

Serpentines.—Among the serpentines, antigorite is the dominant polymorphic form. As identified by X-ray powder pattern, it is 7 Å orthoantigo-

TABLE IV

Chemical compositions of chlorites

		59	61	64	65
SiO_2	..	26·71	39·20	54.05	31.09
TiO_2	..	..	..	..	..
Al_2O_3	..	21·85	9.31	18·82	19·62
Fe_2O_3	..	0·08	0.00	0·34	1·23
FeO	..	14·76	5.75	7·60	6·55
MnO	..	0·03	0.04	0·10	0·13
MgO	..	24·30	34·27	27·63	28·95
CaO	..	..	0.28	..	0·41
Na_2O	..	0·08	0·02	0·51	0·62
K_2O	..	0·01	..	0·10	0·31
H_2O^+	..	12·09	11·19	10·58	10·21
H_2O^-	..	0·12	0·00	0·40	0·57
Total	..	100·03	100·06	99·13	99·69
Number of ions on the basis of 36 (0) atoms					
Si	..	5·307	7·488	6·617	6·139
Al^4	..	2·692	0·512	1·383	1·861
Al_6	..	2·424	1·583	2·926	2·704
Ti	..	..	..	..	..
Fe^{3+}	..	0·012	..	0·050	0·183
Fe^{2+}	..	2·453	0·919	1·235	1·082
Mn	..	0·005	0·007	0·016	0·022
Mg	..	7·198	9·757	8.004	8·522
Ca	..	..	0·057	..	0·087
Na	..	0·031	0·007	0·192	0·237
K	..	0·002	..	0·025	0·018
(OH)	..	16·04	14·27	13·72	13·46

59. M_8 Flaky chlorite, Mangalapur.
61. M_{36} Fine grained chlorite, from the vicinity of Ultramafite, Mangalapur.
64. D_{96} Chlorite associated with anthophyllite, Dodkadanur.
65. D_{76} Chlorite associated with tremolite, Dodkadanur.

TABLE V

Chemical compositions of Garnets

	92	95	97	99	100
SiO_2	37·40	37·05	38·09	36·20	36·70
TiO_2	0·28	0·91	1·27	1·01	..
Al_2O_3	20·65	19·11	20·84	21·35	20.68
Fe_2O_3	0·54	3·80	2·93	2·44	0·32
FeO	27·54	31·62	28·97	28·56	38·89
MnO	3·79	1·62	1·37	0·44	0·71
MgO	3·12	4·43	5·03	3·22	1·40
CaO	6·64	1·66	1·48	6·72	1·42
Total	99·40	100·20	99·98	99·94	100·12
Alm	60·6	63·2	67·0	61·7	89·8
And	1·0	..	9·2	7·1	1·0
Gros	17·7	..	0·0	17·9	2·9
Pyr	12·1	15·8	20·6	12·4	4·7
Spes	8·5	..	3·2	0·9	1·7

92. M_{18} Garnet from amphibolite, Mangalapur.
95. Ygt Garnet with chlorite, Yenneholeranganabetta, Tirumalapur.
97. Bch Garnet associated with chlorite, Biranahalli.
99. I_7 Garnet from amphibolite, Idegondanahalli.
100. Kgt Garnet from kyanite-staurolite schist, Mangalapur.

rite. They have nearly constant composition corresponding to the formula, $Mg_3[Si_2O_5(OH)_4]$ (Table VI). Alumina content upto 4·0 wt% has been observed, where the Al occupies mostly the octahedral sites. Limited substitution of magnesium by ferrous iron takes place as indicated by the FeO concentration ranging from 1·0 to 4·0 wt%. Mg/Mg + Fe in antigorite is more than that of olivine. However, the determination of FeO can be somewhat erroneous due to the inclusions of magnetite. MnO content is extremely low. All the Ni present in olivine is retained in the serpentines.

Carbonates.—Magnesite and dolomite are the only two carbonate phases in ultramafites and TAAC schists. Pure magnesite is found as a surface alteration product. Magnesite associated with anthophyllite asbestos and ultramafites are Fe-rich and is called breunnerite. CaO content is very low in them (Table VI). Dolomite is found in Mangalapur outcrops, which are associated with TAAC schists. It contains larger amount of FeO (2–4%). Mg/Ca ratio in dolomite is more than unity, indicating higher temperature of formation.

Talc.—Minimum substitution is observed in talc such that constant composition is maintained by this mineral corresponding to the formula, $Mg_3Si_4O_{10}(OH)_2$. FeO, Al_2O_3 and MnO in talc are found to be extremely low (Table VI). Talc occurs restricted to those horizons containing anthophyllite and carbonate.

Staurolite.—The composition of staurolite conforms to the general formula $(Fe, Mg)_2Al_4Si_2O_{11}(OH)_2$, with Mg/Mg + Fe ratio 0·1 to 0·15. Titania content varies from 0·80 to 1·5 wt%. They are poor in MnO as the case of garnets from metapelites. Staurolite crystals occasionally found in chlorites of TAAC schist, along with kyanite, show little compositional variation when compared to those coexisting with kyanite, garnet and quartz (metapelites).

Kyanite—Kyanite is predominantly the blue variety, with constant composition corresponding to Al_2SiO_5 (Table VII). Fe_2O_3 is the major impurity, ranging from 0·5 to 0·8 wt%. H_2O^+ content is less than 0·3%.

Plagioclase feldspar.—Plagioclase from the amphibolites contain usually higher CaO content (Table VIII). The end member composition ranges from An_{40} to An_{60}, Ab_{60} to Ab_{40} and $Or_{0\cdot3}$ to $Or_{1\cdot0}$. Higher range of anorthite content in plagioclase from amphibolites is suggestive of high pressure metamorphism. Compositional range of plagioclase from garnetiferous and non-garnetiferous amphibolites overlap.

TABLE VI

Chemical composition of minerals associated with ultramafic rocks

		42	42.*a*	42.*b*	43	47	53	56	51
SiO_2	..	40·33	41·11	39.28	42·36	40·38	..	..	59·70
TiO_2	..	0·05	..	..	..	..	..	..	..
Al_2O_3	..	1·02	0·92	0·87	3·91	1·21	..	..	1·32
Fe_2O_3	..	0·14	0·09	0·19	0·12	1·30	..	..	1·79
FeO	..	12·21	9·23	15·92	2·30	4·26	9·73	2·31	0·51
MnO	..	0·04	0·03	0·04	0·03	..	0·09	0·12	traces
MgO	..	46·16	49·02	42·31	37·71	38·92	40·15	23·91	31·85
CaO	..	..	..	..	0·28	0·83	0·26	23·01	..
Na_2O	..	0·03	..	..	0·82	0·32	..	..	0·12
K_2O	..	..	..	..	0·17	0·01	..	..	0·08
H_2O^+	..	0·15	0·10	0·20	12·12	13·12	..	..	4·62
H_2O^-	..	..	..	..	0·40	0·31	..	..	..
CO_2	..	..	..	..	..	..	49·82	50·05	..
Total	..	100·18	100·48	99·51	100·22	100.66	100·05	99·40	99·99
Si	..	0·997	0·995	1·008	1·979	1·944	..	..	7·658
Al^+	..	0·000	0·005	..	0·021	0·056	..	..	0·1999
Al^6	..	0·030	0·021	0·026	0·194	0·075	..	..	..

Ti	0·001	..	..	..	..	..	..	..
Fe^{3+}	0·003	..	0·001	0·006	0·090	..	..	0·017
Fe^{2+}	0·253	0·187	0.336	0·090	0·164	0·239	0·057	0·055
Mn	0·001	..	..	0·120	..	0·002	0·000	..
Mg	1·702	1·770	1·588	2·628	2·669	1·757	1·048	6·008
Ca	0·000	..	..	0·014	0·040	0·000	0·725	..
Na	..	..	..	0·074	0·028	..	..	0·024
K	..	..	..	0·001	..	..	..	0·013
(OH)	0·020	0·015	0·031	3·782	4·028	..	..	3·953
(CO_2)	..	..	..	..	..	1·997	2·01	..
Fo : Fa	86 : 14	90 : 10	82 : 18	..	..	..	..	..

42. M_0 Olivine, Mangalapur.
42 *a*. Y_0 Olivine, Yenneholeranganabetta, Tirumalapur.
42 *b*. I_0 Olivine, Idegondanahalli.
43. $I_{31\cdot c}$ Chrysotile, Idegondanahalli.
47. OT_A Antigorite, Tirumalapur.
53. $M_{11\cdot B}$ Breunnerite, Mangalapur.
56. D_{24} Dolomite, Dodkadanur.
51. M_T Talc, Mangalapur.

Number of ions are calculated for olivine, chrysotile, antigorite, breunnerite, dolomite and talc on the basis of 4, 9, 9, 6, 6 and 24 oxygen atoms respectively.

TABLE VII

Chemical composition of kyanite and staurolites

	101	102	103
SiO_2	36·89	27·30	28·30
TiO_2	0·02	0·87	1·18
Al_2O_3	61·93	51·98	53·37
Fe_2O_3	0·67	3·02	1·45
FeO	0·05	13·42	12·08
MnO	0·00	0·09	0·17
MgO	0·00	1·28	1·25
CaO	0·00	0·06	0·16
Na_2O	..	..	..
K_2O	..	..	..
H_2O^+	0·31	2·18	2·25
H_2O^-	0·03	0·00	0·03
Total	99·92	100·20	100·25
Si	4·008	7·630	7·807
Ti	0·002	0·183	0·245
Al^+	7·929	17·117	17·321
Fe^{3+}	0·055	0·636	0·300
Fe^{2+}	0·005	3·137	2·782
Mn	..	0·021	0·040
Mg	..	0·537	0·517
Ca	..	0·018	0·050
(OH)	..	4·07	4·14
Mg/Mg + Fe	..	0·079	0·087

101. Kyanite, North of Tirumalapur.
102. Staurolite associated with chlorite-Biranhalli.
103. Staurolite-kyanite-garnet schist, Tattekere,

TABLE VIII

Chemical Composition of Plagioclase feldspar

	104	105	106
SiO_2	53·09	56·01	55·21
Al_2O_3	30·24	28·27	28·38
CaO	12·47	10·05	8·64
Na_2O	4·45	5·80	7·59
K_2O	0·08	0·21	0·08
Total	100·26	100·34	99·85
Number of ions on the basis of 32 (0) *atoms*			
Si	9·576	10·030	9·972
Al	6·412	5·967	6·030
Ca	2·414	1·932	1·674
Na	1·556	2·014	2·644
K	0·018	0·050	0·018
Al	37·60	49·00	56·6
An	62·0	50.0	43·0
Or	0·4	1·00	0·4

104. I_6 From garnetiferous amphibolite, Idegondanahalli.
105. B_5 From garnetiferous amphibolite, Biranahalli.
106. OT From non-garnetiferous amphibolite, Tirumalapur.

4. DISCUSSION

Mineral chemistry studies of anthophyllites, actinolites and chlorites suggests a compositional mixing of more than one rock type in this area leading to the formation of TAAC schist. There can be two different types of mixing:

(i) dunites mixing with pelites and mafites,
(ii) harzburgite-lherzolite types mixing with pelitic rocks.

Occurrence of anthophyllites as segregates and the altered porphyroblasts of pyroxene morphology observed in TAAC schist suggest the mixing to be of the second type. Indeed, the whole rock chemistry supports this. Figure 7 gives the SiCF and ACF diagrams. When the parent rock is a dunite, the composition plots close to Serp-Fo line in the SiCF diagram. With higher magnesite content, it shifts to the F corner. The composition of ultramafites plot in the vicinity of Fo. Harzburgite and lherzolite, with varying ol/ol + opx + cpx ratio, plot anywhere in the Fo-En-Di triangle shaded in Fig. 7 (*a*). Compositions of TAAC schist plot near Di-En line or away, indicating that they are more silica-rich. It is evident from Fig. 7 (*b*) that Al_2O_3, CaO and (MgO + FeO) contents are widely variable in the constituent minerals, suggestive of a mixed rock type. Considering that the ultramafites ranged from dunite to harzburgite to lherzolite, it is surprising that no pyroxene-bearing rocks are preserved unlike the dunites, in spite of the fact that olivines are less stable than pyroxenes. This may be due to the larger size of a few dunite bodies, portions of which remained unmixed.

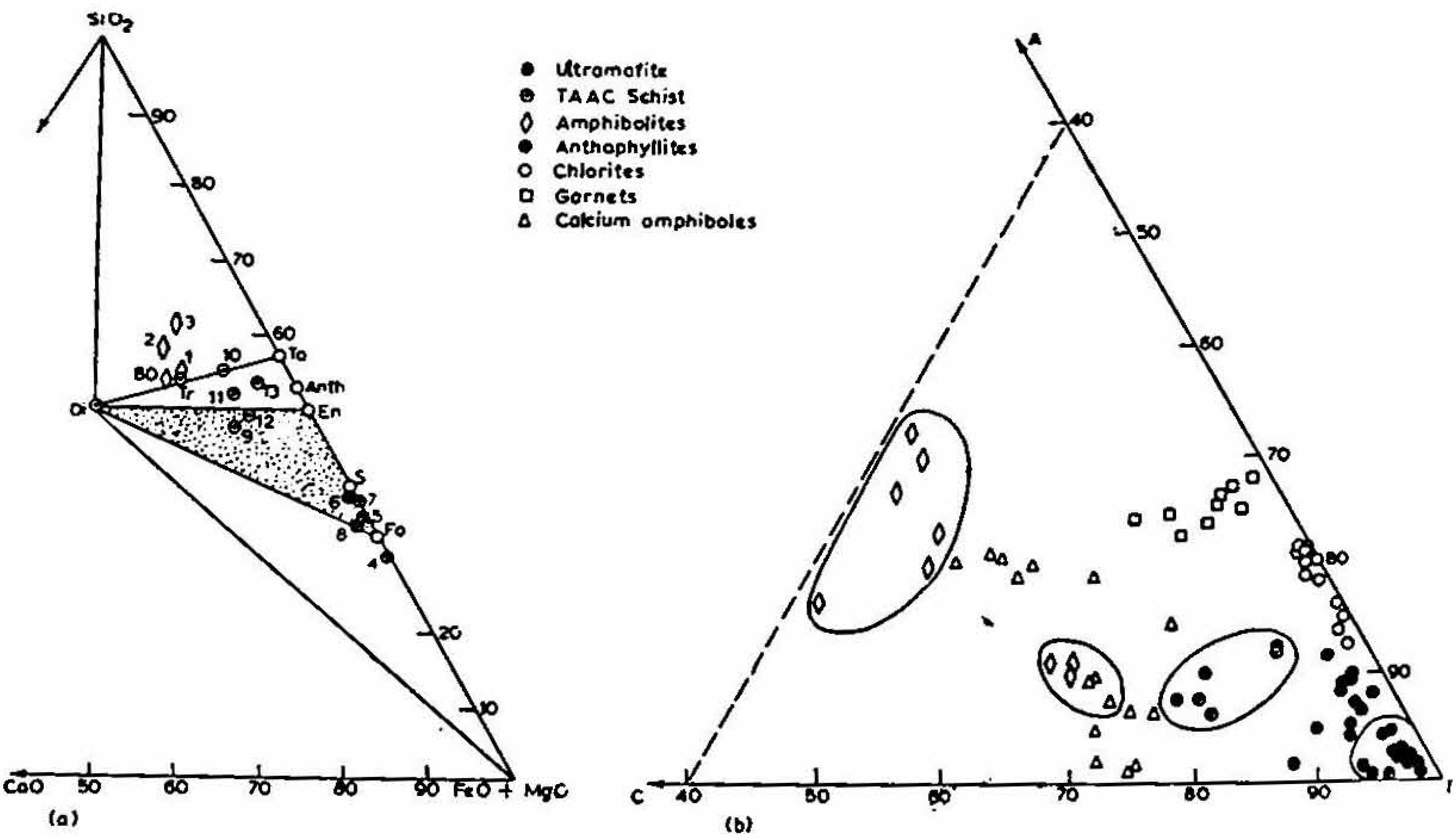

FIG. 7. Compositional variations in ultramafites, amphibolites, TAAC rocks and constituent minerals. (*a*) $SiO_2 - CaO - (FeO + MgO)$, (*b*) $A = Al_2O_3 - (Na_2O + K_2O)$, $C = CaO$, $F = (FeO + MgO + MnO)$.

Metamorphic changes in ultramafites.—Metamorphic changes in ultramafites generate not only hydroxyl bearing minerals but also carbonates from the parent olivine and pyroxenes. SiO_2, MgO and FeO are essential components in the rock, when olivine and enstatite are the major phases present. In lherzolite, Cpx brings CaO as an additional component. Both OPx and CPx may contain some amount of Al_2O_3.

Reactions in which anthophyllite is formed are important for the present discussion. However, the pertinent reactions to be considered must account for the paragenesis ranging from anth, anth + magnesite, anth + serp +ol+ magnesite + magnetite to serp + magnetite + talc + ol. Metamorphism of ultramafites of Central Alps has been investigated by Evans and Trommsdorff [13–16], but differs from the present assemblages in that orthopyroxene, olivine (both secondary) and talc are abundant in the Alps. The observed assemblages in ultramafites can be explained on the basis of experimental work on the system: $MgO\text{-}SiO_2\text{-}CO_2\text{-}H_2O$ by Greenwood [17] and Johannes [18]. Figure 8 gives the two ends of $T\text{–}X_{CO_2}$ plane at constant pressure of 2kb. All the possible reactions in the system are given in this figure. Presence of iron can be taken into account by considering (Fe-Mg) in place of Mg and the occurrence of magnetite can thus be accounted for, during the conversion of olivine to serpentine. Anthophyllite is generated in the lower temperature ranges through a set of reactions when $X_{CO_2} = 0{\cdot}82$ to $0{\cdot}98$ [Fig. 8 (*a*)]. In comparison, serpentine is stable only upto $X_{CO_2} = 0{\cdot}05$ [Fig. 8 (*b*)]. The temperature stability of serpentine is limited by reaction (13). The P–T curve for this reaction indicates that serpentine persists to about 590° C at 10 Kb (Fig. 9).

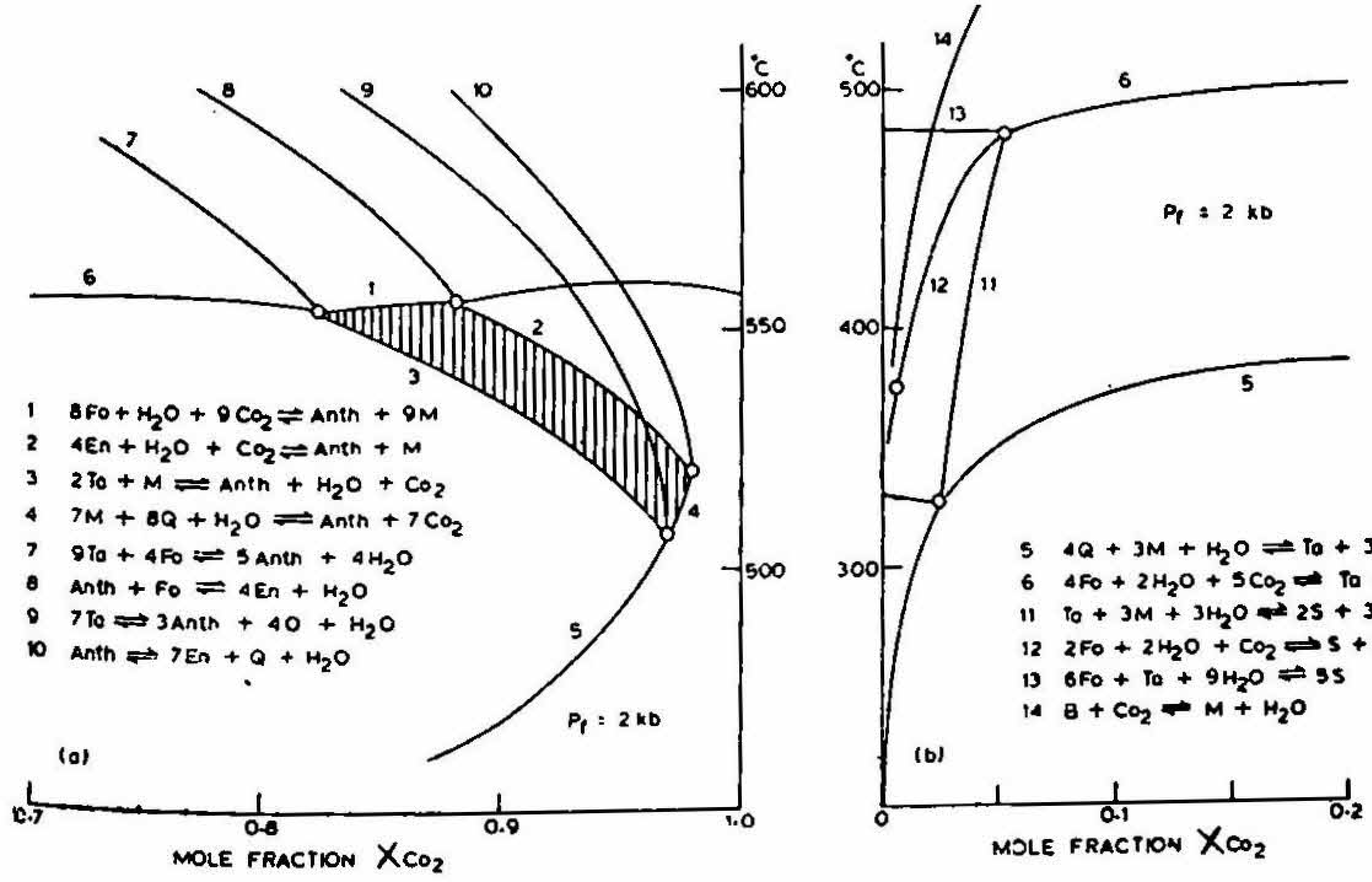

FIG. 8. Isobaric equilibrium curves of reactions occurring at various values in the system $MgO - SiO_2 - CO_2 - H_2O$. Data from Johannes, W. [18]. Anth = Anthophyllite, En = Enstatite, S = Serpentine, Fo = Forsterite, B = Brucite, M = Magnesite, Ta = Talc.

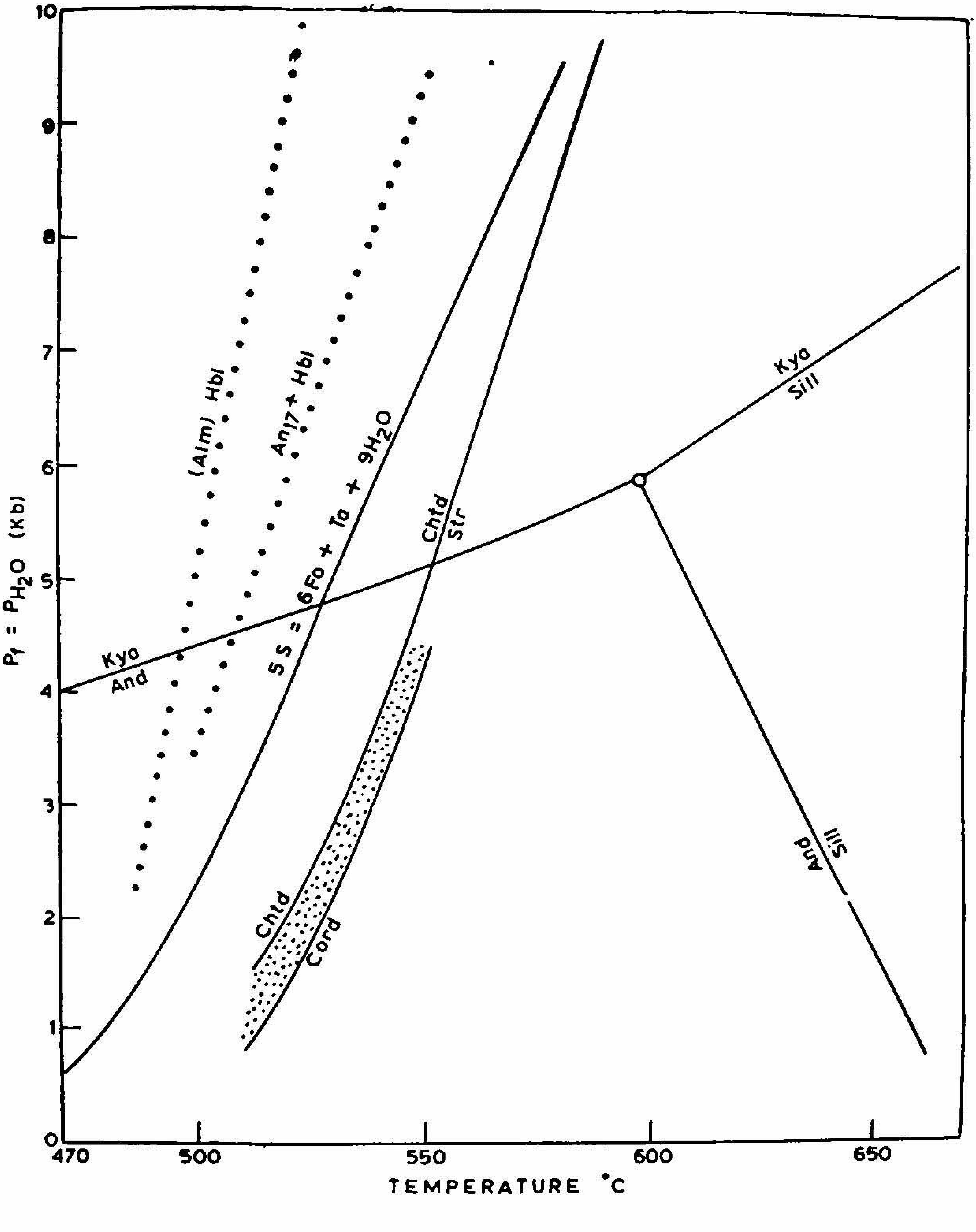

FIG. 9. Pressure-Temperature curves for some of the key reactions. Stability fields of the three polymorphs of Al_2SiO_5 are deliniated. S = Serpentine, Fo = Forsterite, Ta = Talc, Alm = Almandine, Hbl = Hornblende, An = Anorthite, Chtd = Chloritoid, Str = Staurolite, Cord = Cordierite, Kya = Kyanite, Sill = Sillimanite and And = Andalusite

The coexistence of serpentine with anthophyllite can only be explained on the basis of any one of the following conditions : (i) a steep fall in temperature at very low X_{CO_2} value where reaction (7) quickly changes over to reaction (13) or (12), as indicated in Fig. 8, (ii) when P_{H_2O} is of the order of 5 to 8 Kb, the reaction (13) is shifted to 550° to 575° C (Fig. 9). If X_{CO_2} is increased by CO_2 metasomatism, without altering the total pressure, any one of the reactions (1) to (4) may set in, possibly (3). Unfortunately, P–T curves for the reactions under high X_{CO_2} are not available. Presumably, the dT/dp for the anthophyllite forming reaction at $X_{CO_2} = 0.8 - 1{\cdot}0$ is lower than that of reaction (13).

Occurrence of serp + anth as isolated bodies surrounded by anth + carbonates or anth + chl + carbonate rocks; absence of periclase-brucite and brucite-magnesite in thin sections and the presence of anthophyllite as a phase generated (not a disappearing phase) suggests the preference for the second alternative. The distribution pattern of anthophyllite bodies in the field suggest that CO_2 metasomatism did not alter the fluid composition uniformly.

The reactions given in Fig. 8 are to be suitably modified to account for the effect of CaO and Al_2O_3. When diopside is present in lherzolite, reaction (2) can be rewritten as:

$$5MgSiO_3 + 2\,(Ca_{0\cdot5}Mg_{0\cdot5})\,SiO_3 + Mg_2SiO_4 + 2CO_2 + H_2O \rightarrow Mg_7Si_8O_{22}(OH)_2 + (Ca,\ Mg)\ CO_3 \qquad (15)$$

This reaction is further modified to account for the formation of tremolite, $Ca_2Mg_5Si_8O_{22}(OH)_2$, in place of anthophyllite. When the concentration of Al_2O_3 is high, chlorite is formed in preference to talc and serpentine. However, the composition of chlorite varies depending upon the alumina present in pyroxene or that introduced from the metapolites. In the hybrid rocks, the most general reaction is:

$$8MgSiO_3 + 6Mg_2SiO_4 + 2CaMgSi_2O_6 + 2Al_2SiO_5 + 2SiO_2 + 10H_2O \rightarrow Ca_2Mg_5Si_7O_{22}(OH)_2 + 2Mg_5Al\,(Si_3Al)O_{10}(OH)_8 + Mg_7Si_8O_{22}(OH)_2 \qquad (16)$$

Since the number of phases involved are eight, it is preferable to split this reaction to a number of parallel ones, involving less number of phases. This will account for the paragenesis in the TAAC schist. Carbonates as additional phases which indicate higher X_{CO_2} in restricted horizons of the area. The condition of formation of tremolite and chlorite compare with those of anthophyllite in the ultramafites.

Garnets coexisting with chlorites are in apparent equilibrium and can be regarded as the product of reaction.

Chlorite + Quartz → Garnet + Water (17)

P–T Conditions of Metamorphism.—The metamorphic changes in the ultramafites indicate a higher pressure (5–8 Kb) and medium temperature (500–600° C). The mineral assemblages in the other rock types also suggest persistence of nearly the same P–T conditions. In the metapelites, chlorite chloritoid-garnet (found in the northern portions) change over to kyanite-staurolite-garnet in the southern region. According to Winkler [19], this indicates upper green schist changing over to the lower amphibolite facies. Absence of cordierite and presence of garnet along with kyanite corresponds to higher pressures. In the absence of muscovite, staurolite is produced only by the reactions:

Chlorotoid + kyanite → staurolite + quartz + H_2O (18)

Chlorotoid + quartz → staurolite + almandine + H_2O (19)

These reactions are experimentally found to take place in the temperature range of 525 to 570° C and pressure of 4–8 Kb, the composite P–T curves being given in Fig. 9 (Hoschek [20]; Richardson [21]; Ganguly [22]). The mineral assemblages in the apmhibolites, cannot be used as indicators for the estimation of exact P–T conditions because of the wide range of compositions of the dominant phases in them, namely, plagioclase and hornblende. The sudden change of plagioclase composition from albiclase to oligoclase-andesine, coexisting with hornblende is said to indicate the transition from greenschist to amphibolite. The estimated P–T curves are presented in Fig. 9 (Wenk and Keller [23], Turner [24]).

The plagioclase composition is more than andesine, ranging upto bytownite, coexisting with tschermakite-pargasitic hornblende, garnets from the amphibolites being pyrope-grossular containing almandine. These criteria are indicative for pressures corresponding to the kyanite stability field (> 5 Kb), in the temperature region corresponding to lower amphibolite.

The persistence of chlorite in the amphibolite grade of metamorphism is not uncommon, because Mg-rich chlorite remains stable in the absence of muscovite. P–T conditions experienced by chlorites are not different from those of metapelites as indicated by the presence of kyanite and staurolite in them. Thus the conditions of metamorphism estimated from the paragenesis of different rock types indicate the transition from upper greenschist to lower amphibolite grade (520–570° C) and medium pressure (5–8 Kb). However, it is evident that the temperature corresponding to talc + Fo = anth or talc + Enst=Anth has never been reached at any given X_{co_2} value. These assemblages are characteristically present in the metamorphosed ultramafites of Central Alps, which Evans and Trommsdorff [13–16] have placed within the amphibolite facies.

Origin of Asbestos in the Area.—As mentioned earlier, anthophyllite is the most predominant variety of asbestos in the area. Except for the minor constituents, there is no difference betwen asbestiform and massive, crystalline anthophyllite, with respect to major constituents and X-ray crystal structures. Therefore, the asbestiform is only a morphological variant. Two important factors influence the morphology of crystals: (i) impurities present in the environment of crystallisation and (ii) physical conditions like differential temperature and directional pressure. The mineral chemistry studies indicate that the minor constituents like CaO, Al_2O_3 and alkali are low in the asbestiform anthophyllite. Evidently, these constituents should be a minimum in the environment of formation of asbestos. It has also been observed that asbestiform anthophyllite has comparatively lower Mg/Mg + Fe ratio, when compared to the adjoining massive variety or ‘ mountain wood ’ type.

Asbestos occurs in certain horizons as thick veins and these veins are not uniformly distributed in the ultramafites. Some of the thick veins have strike perpendicular to that of the adjoining TAAC schist. In many a place, they are associated with carbonates, where sheaves of fibrous anthophyllite are found developed within the carbonates. The veins contain woody type of anthophyllite which according to the X-ray studies are only partially crystallised. Often, relict nodules are found within the asbestos veins which has serpentine, talc, talc-chlorite and magnesite as minerals. These observations can only be explained on the basis that asbestos is derived through recrystallisation of ultramafic rocks in presence of a fluid phase of comparatively higher (but variable) X_{co_2} values, towards the waining stages of metamorphism. The approximate conditions of crystallisation of anthophyllite is borne out from the phase equilibrium studies, according to which, anthophyllite has limited range of stability and cannot be formed below 500° C, whatever may be the X_{CO_2} values. The veins may be restricted to shear or fracture zones in which the residual fluid must have accumulated. Such later growth of anthophyllite (not asbestiform) has been reported from Alps by Evans and Trommsdorff [16]. The influence of directional pressure can be expected as additional factor for the formation of anthophyllite asbestos, direct evidences are, however lacking.

5. ACKNOWLEDGEMENT

The authors are thankful to Prof. A. R. V. Murthy for his kind encouragement. They are indebted to Mr. N. Ranganatha Rao, S.L.N. Mines, Holenarasipur, for providing facilities during field work. R.V.R. expresses gratitude to C.S.I.R., India, for the award of a fellowship.

REFERENCES

[1] Anantha Iyer, G. V., Narayanan Kutty, T. R. and Raghavendra, R. V. *Curr. Sci.*, 1974, **43**, 402.

[2] Sampath Iyengar, P. .. *Mysore Geol. Dept. Rec.*, 1910, **11**, 82.

[3] Rama Rao, B. .. *Mysore Geol. Dept. Rec.*, 1924, **21**, 146.

[4] Rama Rao, B. .. *Mysore Geol. Dept. Rec.*, 1925, **22**, 146.

[5] Venkataramanayya, S. *Mysore Geol. Dept. Rec.*, 1909, **10**, 88.

[6] Wilson, A. D. .. *Bull. of Geol. Survey*, Great Britain, 1955, **9**, 56.

[7] Deer, W. A., Howie, R. A. and Zussman, J. *Rock Forming Minerals*, Longman, London, 1963, **2**, 272.

[8] Leake, B. E. .. *Geol. Soc. Amer. Spec. Pap.*, 1968, **98**, 210.

[9] Kostuk, E. A. and Sobolev, V. S. *Lithos*, 1969, **2**, 67.

[10] Hey, M. H. .. *Min. Mag.*, 1954, **30**, 277.

[11] Velde, B. .. *Min. Mag.*, 1973, **39**, 297.

[12] Simkin, T. and Smith, J. V. *J. Geol.*, 1970, **78**, 304.

[13] Evans, B. W. and Trommsdorff, V. *Schweiz Mineral. Petrogr. Mitt.*, 1970, **50**, 481.

[14] Trommsdorff, V. and Evans, B. W. *Amer. J. Sci.*, 1970, **272**, 423.

[15] Trommsdorff, V. and Evans, B. W. *Schweiz, Mineral. Petrogr. Mitt.*, 1974, **54**, 333.

[16] Evans, B. W. and Trommsdorff, V. *Amer. J. Sci.*, 1974, 274, 274.

[17] Greenwood, H. J. .. *J. Petr.*, 1963, 4, 317.

[18] Johannes, W. .. *Amer. J. Sci.*, 1969, 267, 1083.

[19] Winkler, H. G. F. .. *Petrogenesis of Metamorphic Rocks*, Springer-Verlag, Heidelberg, 1974, pp. 74-93 and 160-164.

[20] Hoschek, G. .. *Contr. Mineral. Petrol.*, 1967, 14, 123.

[21] Richardson, S. W. .. *J. Petr.*, 1968, 9, 467.

[22] Ganguly, J. .. *Amer. J. Sci.*, 1969, 267, 910.

[23] Wenk, C. and Keller, F. *Schweiz. Mineral. Petrogr. Mitt.*, 1969, 49, 157.

[24] Turner, F. J. .. *Metamorphic Petrology*. McGraw-Hill Book Co., New York, 1968.